Effect of mixing structure on the water uptake of mixtures of ammonium sulfate and phthalic acid particles

Weigang Wang[1,4†], Ting Lei[2,3†], Andreas Zuend[5], Hang Su[3], Yafang Cheng[2], Yajun Shi[1], Maofa Ge[1,4,6], Mingyuan Liu[1,4]

[1]State Key Laboratory for Structural Chemistry of Unstable and Stable Species, CAS Research/Education Center for Excellence in Molecular Sciences, Institute of Chemistry, Chinese Academy of Sciences, Beijing 100190, PR China

[2]Minerva Research Group, Max Planck Institute for Chemistry, Mainz 55128, Germany

[3]Multiphase Chemistry Department, Max Planck Institute for Chemistry, Mainz 55128, Germany

[4]University of Chinese Academy of Sciences, Beijing 100049, PR China

[5]Department of Atmospheric and Oceanic Sciences, McGill University, Montreal, Quebec, Canada

[6]Center for Excellence in Regional Atmospheric Environment, Institute of Urban Environment, Chinese Academy of Sciences, Xiamen 361021, PR China

† These authors contributed equally to this work

Correspondence to: Weigang Wang (wangwg@iccas.ac.cn) and Maofa Ge (gemaofa@iccas.ac.cn)

Abstract. Aerosol mixing state regulates the interactions between water molecules and particles and thus controls the aerosol activation and hygroscopic growth, which thereby influences the visibility degradation, cloud formation, and its radiative forcing. Current studies on the mixing structure effects on aerosol hygroscopicity, however, are few reported. Here, we investigated the hygroscopicity of AS/PA aerosol particles with different mass fractions of PA in the different mixing states in terms of initial particle generation. Firstly, effect of phthalic acid (PA) coatings on the hygroscopic behavior of the core-shell-generated mixtures of ammonium sulfate (AS) with PA has

been studied using a coating-hygroscopicity tandem differential mobility analyzer (coating-HTDMA). The slow increase in the hygroscopic growth factor of core-shell-generated particles is observed with increasing thickness of coating PA prior to DRH of AS. At RH above 80 %, a decrease in hygroscopic growth factor of particles occurs as the thickness of PA shell increases, which indicates that the increase of PA mass fractions leads to a reduction of the overall core-shell-generated particle hygroscopicity. In addition, the use of the ZSR relation leads to the underestimation of the measured growth factors of core-shell-generated particles without consideration of the morphological effect of core-shell-generated particles, especially at higher RH. Secondly, in the case of the AS/PA initially well-mixed particles, a shift of deliquescence relative humidity (DRH) of AS (~80 %, Tang and Munkelwitz (1994)) to lower relative humidity (RH) is observed due to the presence of PA in the initially well-mixed particles. The predicted hygroscopic growth factor using the ZSR relation is consistent with the measured hygroscopic growth factor of the initially well-mixed particles. Moreover, we compared and discussed the influence of mixing states on the water uptake of AS/PA aerosol particles. It is found that the hygroscopic growth factor of the core-shell-generated particles is slightly higher than that of the initially well-mixed particles with the same mass fractions of PA at RH above 80 %. The observation of AS/PA particles may contribute to a growing field of knowledge regarding the influence of coating properties and mixing structure on water uptake.

1 Introduction

The ability of aerosol particles to absorb and maintain water molecules, called hygroscopicity, is one of the most important physicochemical properties of atmospheric aerosol particles with

46 profound implications (Shi et al., 2012; Lei et al., 2014, 2018; Gupta et al., 2015; Hodas et al., et
47 al., 2015; Zawadowicz et al., 2015; Martin et al., 2017). It might determine the phase state (Mu et
48 al., 2018), size (Peng et al., 2001; Choi et al., 2002), mixing state, optical properties, and chemical
49 reactivity of atmospheric aerosols exposed to the environment of the different RHs (Heintzenberg
50 et al., 2001; Rudich et al., 2003; Spindler et al., 2007; Abo Riziq et al., 2007, 2008; Eichler et al.,
51 2008). Moreover, the change of these properties after water absorption on aerosol particles can
52 strongly affect the cloud formation, aerosol radiative forcing, global climate, and even human health
53 (Cheng et al., 2008; Reutter et al., 2009; Rose et al., 2011; Stock et al., 2011; Liu et al., 2012, 2013;
54 Tie et al., 2017). Therefore, the interaction between water molecules and aerosol particles is crucial
55 for a better understanding of the aerosol-cloud-climate effects in the atmosphere (Sjogren et al.,
56 2007; Zamora et al., 2011; Jing et al., 2016).
57 Atmospheric aerosols contain a complex mixture of inorganic and organic compounds in the
58 different mixing structures, e.g., externally mixed, internally mixed (Ganguly et al., 2006). The
59 internally well-mixed aerosol particles may be divided into homogeneous and heterogeneous
60 internally mixed aerosol particles (Lang-Yona et al., 2009), which could, in turn, strongly influence
61 the water uptake, optical properties, and the cloud condensation nuclei (CCN) ability of the particles
62 (Lesins et al., 2002; Falkovich et al., 2004; Zhang et al., 2005; Schwarz et al., 2006; Su et al., 2010).
63 Most of the previous studies on the hygroscopic behavior of multi-components aerosol focus on the
64 well-mixed particles generated from internally mixed solutions (Miñambres et al., 2010; Shi et al.,
65 2014; Gupta et al., 2015; Jing et al., 2016; Lei et al., 2014; 2018). For example, Choi and Chan
66 (2002) studied on the effects of glycerol, succinic acid, malonic acid, citric acid, and glutaric acid
67 on the hygroscopic properties of sodium chloride and AS in the initially well-mixed aerosol particles,

68 respectively, using an electrodynamic balance. They observed that the deliquescence and
69 efflorescence of sodium chloride and AS were affected by the presence of different organic
70 components in the mixed aerosol particles. Concerning the hygroscopicity of the heterogeneity of
71 internally mixed aerosol particles, such as core-shell particles, there are several studies on
72 investigating their interaction with water molecules (Ciobanu et al., 2009; Song et al., 2012;
73 Shiraiwa et al., 2013; Hodas et al., 2015; Song et al., 2018). However, to date, few laboratory studies
74 have been investigated on the influence of organic coatings on the hygroscopic behavior of core-
75 shell particles and the difference of mixing state effects on the hygroscopicity of aerosol particles
76 (Zhang et al., 2008; Pagels et al., 2009; Xue et al., 2009; Lang-Yona et al., 2010; Ditas et al., 2018).
77 E.g., hygroscopicity tandem differential mobility analyzer (HTDMA) study on the organic coating
78 effects on the hygroscopicity of core-shell aerosol particles was studied by Maskey et al. (2014).
79 They observed a shift of DRH of AS to lower RH for the core-shell particles due to presence of
80 levoglucosan coatings. They further compared water absorption on AS/levoglucosan core-shell
81 particles and the AS/succinic acid core-shell particles. They suggest that different organic coatings
82 lead to changes in the hygroscopic properties of core-shell particles. Chan et al. (2006) investigated
83 hygroscopicity of AS coated with different mass fractions of glutaric acid during two continuous
84 humidification and dehumidification cycles using a Raman spectra and an electrodynamic balance.
85 They observed different hygroscopic behavior and morphology of aerosol particles between the two
86 humidification and dehumidification cycles due to the different mixing states. Therefore, to
87 investigate organic coating effect on the hygroscopicity of aerosol particles and further to study on
88 difference of mixing states effects on the hygroscopic behavior of aerosol particles are crucial for
89 estimation the direct and indirect radiative effect of aerosol particles on the Earth's climate (Saxena

et al., 1995; Ansari et al., 2000; Maskey et al., 2014).

PA is ubiquitous in rural mountains and marine atmosphere in Asia (Wang et al., 2011). It is mainly produced by the photo-oxidation of volatile organic compounds (VOCs), such as xylene, and naphthalene (Kawamura and Ikushima, 1993; Schauer et al., 1996; Zhang et al., 2016). Also, PA has been identified as a significant contributor to the urban organic compounds (Rogge et al., 1993). PA particles are generally used as a tracer for the secondary organic aerosol (SOA) in atmospheric fine particles (Schauer et al., 2000, 2002). Furthermore, these aromatic acids like PA, which are photo-oxidation products of anthropogenic precursors such as toluene, xylene, and naphthalene, are initially formed as gaseous products and subsequently condensed onto pre-existing particles. Also, Kleindienst et al. (1999) investigated that hygroscopic particles formed after irradiating toluene, p-xylene, and 1,3,5-trimethylbenzene in the presence of NOx and AS seed in a chamber. This suggests the likely existence of PA in atmospheric aerosol particles. Organic coatings on inorganic aerosol particles in the atmosphere can play an important role in the range of RHs over which particle-bound water influences aerosol properties, such as the overall density, the light scattering behavior and the refractive index. Recently, Zhang et al. (2016) reported the importance of atmospheric PA aerosol particles in the visibility degradation and the formation of CCN. The organic PA can have a profound effect on light scattering, hygroscopictiy, and phase transition properties of multicomponent atmospheric aerosols. However, these physicochemical properties of PA have been little documented in the literature (Brooks et al., 2004; Liu et al., 2016). Here, we summarized a few studies on the hygroscopicity of the PA-containing aerosol particles. Brooks et al. (2004) investigated continuous hygroscopic growth of PA aerosol particles in the humidification process using HTDMA technique. Hori et al. (2003) and Huff Hartz et al. (2006) measured the high CCN

activity of PA in spite of its low solubility. Also, liquid-liquid phase separations (LLPS) with aerosol particles consisting of organic and inorganic components was observed by many groups (Ciobanu et al., 2009; Betram et al., 2011; Song et al. 2012a, 2012b; You et al., 2014). For example, Song et al. (2012a, 2012b) investigated that LLPS occurs in the mixed dicarboxylic acids containing 5, 6, and 7 carbon using an optical microscopy and micro-Raman spectroscopy, and further established that occurrence of LLPS of aerosol particles has an average elemental oxygen-to-carbon (O:C) ratio of the organic fraction of less than 0.8. Subsequently, the occurrence of liquid-liquid phase separation in the internally mixed aerosols consisting of AS and PA was performed by Zhou et al. (2014) during the dehumidification processes using a Raman spectra. You et al. (2014) further found that the LLPS of aerosol particles with a different O: C ratio of 0.5<O: C<0.8 depends on the types of organic functional groups and inorganic salts presented. Therefore, these studies suggest that the LLPS in the mixed organic and inorganic components aerosol particles is influenced by the amounts of organic and inorganic aerosol components and types.

In this work, AS is chosen as a test substance because it is a major component of the atmospheric aerosol and its thermodynamic behavior is well characterized. Most importantly, ammonium sulfate particles are stable and not volatile, useful features for HTDMA studies. We investigated the effect of the different thickness of coating PA and the AS core size on the water uptake of core-shell-generated particles, and further studied the effect of the mixing states on the hygroscopic behavior of PA /AS aerosol particles using HTDMA technique. For example, we compared the hygroscopic behavior of initially well-mixed AS/PA particles with that of core-shell-generated AS/PA particles with the same PA mass fractions. In addition, we used the Zdanovskii-Stokes-Robinson (ZSR) relation to predict the hygroscopic growth factor (GF) of mixed aerosol particles in the different

mixing structure. Moreover, the Aerosol Inorganic-Organic Mixtures Functional groups Activity Coefficients (AIOMFAC) model (Zuend et al., 2008; 2011) with a version of the liquid-liquid equilibrium (LLE) algorithm was employed in our study to predict the phase compositions of liquid and solid phases for a given composition of a mixture (Zuend and Seinfeld. 2013).

2 Experimental and modeling methods

2.1 HTDMA setup and experimental protocol

HTDMA setup is employed to measure the aerosol nanoparticle hygroscopic growth factor (g_f) and phase transition in the RH range from 5 % to 90 %. Here, g_f is defined as the ratio of mobility diameter of aerosol particles after humidification (D_m(RH)) to that dry condition (D_m (<5 % RH)). Figure 1 shows a schematic diagram of the HTDMA setup. It is comprised of four main components, including three differential mobility analyzers (DMA), a condensation particle counter (CPC), a humidification system, and a coating system. The more detailed information on the HTDMA setup, calibration, and verification have been described elsewhere (Lei et al., 2014; 2018; Jing et al., 2016; Liu et al., 2016). In our study, the particle-sizing, the aerosol/sheath flow rates, and DMA voltage supply have been calibrated every month, respectively. The uncertainty of aerosol/sheath flow rates are kept within ±1% around the reference values. The deviations of the measured DMAs voltage from set-point values is less than ±1%. The sizing agreement of DMAs between the measured diameter of polystyrene latex (PSL) spheres and their nominal diameter (100±3 nm) is within ±1%. Thus, the calculated uncertainty of growth factor depends on the error propagation formula by $\sqrt{\left(\left(g_f \frac{\sqrt{2}\varepsilon_{Dp}}{D_p}\right)^2 + \left(\varepsilon_{RH} \frac{dg_f}{dRH}\right)^2,\right)}$ (Mochida and Kawamura, 2004). Here, ε_{Dp}, ε_{RH}, and g_f are uncertainty of particle mobility diameter, relative humidity, and growth factor at different RH, respectively. The average sizing offsets of our system is taken here as $\frac{\varepsilon_{Dp}}{D_p}$. Also, the RH uncertainty is the accuracy of RH sensor (±2 %). In this study, the calculated uncertainty of growth factor of AS/PA aerosol particles is ~1%-2%. The chemical substances and related to physical properties are available in the Supporting Information Table S1. The solutions used in our measurements are

prepared with distilled and de-ionized Milli-Q water (resistivity of 18.2 MΩ cm at 298 K).

2.1.1 Initially well-mixed AS/PA Aerosol particles

Briefly, poly-disperse aerosol particles were atomized from homogeneous bulk solutions with different mass fractions of PA and AS (Fig. 1), assuming that the compositions of aerosol particles remain the same as that of the solutions used in the atomizer (MSP 1500, MSP). Due to morphology and mixing state of AS/PA aerosol particles generated by an initially well-mixed aqueous solution as indicated by Fig. S2 at dry RH, note that aerosol particles generated this way are referred to as initially well-mixed aerosol particles. The resulting particles were dried and subsequently charged through a dryer and then a neutralizer, respectively. A mono-disperse distribution of particles with a desired diameter were selected by the first differential mobility analyzer (DMA1) with RH below 5 %. After particle sizing, the aerosol particles were exposed to a humidification mode (5 %→90 %) in the Nafion conditioner tubes. The number size distributions of humidified aerosol particles were then measured by a DMA3 coupled with a CPC. To have a precise control of the aerosol RH, the flow rates of the humid and dry air were adjusted with a proportional-integral-derivative (PID) system. Also, to ensure the sufficient water equilibrium with aerosol particles, the difference between RH2 and RH3 (RH in the sheath flow) was within 2 % during the experiment.

2.1.2 Core-shell-generated AS/PA aerosol aerosols

The AS core aerosol particles were generated from an aqueous solution of AS (0.05 wt %) by an atomizer. After a passage through a silica gel diffusion dryer and a neutralizer, the AS core aerosol particles with a certain diameter (100, 150, and 200 nm, respectively) were firstly selected by a DMA1 and then exposed to organic vapors in a coating system. To be specific, the coating system contains a controlled silicone oil bath vaporizer, a reservoir of organic compound, and a condenser.

The AS core particles passed through a sealed flask immersed in a silicone oil bath. The sealed flask was filled with the PA powder. The PA vapors were enriched into the aerosol flow by heating. The temperature required for vaporizing PA is between ~100 and ~130°C, which corresponds to coating thickness between 10 and 50 nm. The resulting organic vapors were condensed onto the AS core particles after cooling to an ambient environment through a condenser. Similarly, this system for coating organic components on the particles has been proved to be efficient by Abo Riziq et al. (2008). The coated particles of a certain size were then selected by the DMA2 to determine the thickness of organic components ($D_{total} = D_{core} +$ coating). After core-shell-generated particle-sizing, aerosols were pre-humidified in a Nafion tube and flowed into the second Nafion humidifier at the set RH2 to reach equilibrium for growth of aerosol particles. Finally, the humidified core-shell-generated particles were detected by a DMA3 and a CPC at ambient temperature. The uncertainty of thickness of coating PA is ± 1.0 nm, considering the fluctuation in temperature and uncertainty of sizing measurements by DMAs. Due to morphology and mixing state of AS/PA aerosol particles generated by a coating-HTDMA at dry RH, note that aerosol particles generated this way are referred to as core-shell-generated aerosol particles.

2.2 Theory and modeling methods

2.2.1 GF data fit

We use the following expression to predict the hygroscopic growth factor of individual components.

$$GF = \left[1 + (a + b * a_w + c * a_w^2)\frac{a_w}{1-a_w}\right]^{\frac{1}{3}} \quad (1)$$

Here it is assumed that water activity (a_w) is equal to the water saturation ratio (a_w = RH / 100 %). The coefficients a, b, and c are determined by fitting Eq. (1), and their values are shown in Table 1 according to the measured GF data against RH. The equation (1) is expected to fit the continuous

water uptake behavior of particles (Brooks et al., 2004; Kreidenweis et al., 2015).

2.2.2 GF predictions by ZSR

We use the Zdanovskii-Stokes-Robinson (ZSR) relation to calculate the hygroscopic growth factor of mixed particles, GF_{mixed}. The GF of a mixture can be estimated from the GF_j of the pure components j and their respective volume fractions, ε_j, in the mixture (Malm and Kreidenweis, 1997). R_{As} is radius of core and $R_{core\text{-}shell}$ is radius of core-shell-generated aerosol.

$$\mathrm{GF_{mix}} = \left[\sum_j \varepsilon_j \, (\mathrm{GF_j})^3\right]^{\frac{1}{3}} \quad (2)$$

$$\varepsilon_{AS} = \frac{\frac{4}{3}\pi R_{AS}^3}{\frac{4}{3}\pi R_{core-shell}^3} \quad (3)$$

3 Results and discussion

3.1 Hygroscopic growth of initially well-mixed aerosol particles

Figure 2 shows the measured hygroscopic growth factors of the AS, PA, and initially well-mixed AS with different mass fractions of PA particles with dry diameter 100nm against RH, respectively. During the hydration mode, there is no change in size until a slow increase occurs at 60 % RH in the case of initially well-mixed AS/PA aerosol particles. This increase may occur because the PA uptakes a small amount of water. However, an abrupt increase in the hygroscopic growth factor is observed at 75 % RH for initially well-mixed particles containing 50 and 75 wt % PA, of which the growth factor is higher than that of pure PA aerosol particles (1.09 ± 0.01 nm from measurements shown in Fig. 2) at the same RH. An interesting, yet contrasting phenomenon is that water uptake for initially well-mixed particles containing 50 wt % PA components is relatively higher than that of mixtures containing 75 wt % PA at 75% RH. One possible reason is that the full deliquescence of AS in the initially well-mixed particles with 50 wt % PA components is completed at 75 % RH, while AS in the mixtures containing 75 wt % PA components is partially deliquescent. A decrease

227 in the hygroscopic growth factor of initially well-mixed AS/PA particles with increasing mass
228 fractions of PA is observed at RH above 80 %. For example, the measured growth factors for initially
229 well- mixed aerosol particles containing 25, 50, and 75 wt % PA are 1.36, 1.28, and 1.19 at 80 %
230 RH, respectively, lower than the growth factor of 1.45 for pure deliquesced AS particles (value from
231 measurements shown in Fig. 2) at the same RH. Also, the measured hygroscopic growth factors
232 within experimental uncertainty were in good agreement with the results from the initially well-
233 mixed particles performed by Hämeri et al. (2002). In addition, with increasing mass fractions of
234 PA in the initially well-mixed particles, the smoothing of the hygroscopic growth factor curves is
235 obvious, indicating that the PA aerosol particles have a significant effect on the water uptake of
236 initially well-mixed AS/PA particles such as a shift or suppression of DRH of AS in the mixed
237 particles. For example, in the case of 1:3 mixtures of AS:PA (by mass), 75 wt % PA in the initially
238 well-mixed particles suppresses the deliquescence of AS, i.e., AS in the initially well-mixed
239 particles slowly dissolve into the liquid phase due to continuous water uptake of PA prior to the
240 deliquescence relative humidity of AS (80 % RH). This similar phenomenon was observed by
241 previous studies (e.g., Hämeri et al., 2002; Qiu and Zhang, 2013). For example, Qiu and Zhang
242 (2013) observed that mixture particles consisting of dimethylaminium sulfate and AS exhibited a
243 moderate growth by water uptake in the RH range of 40 %-70 % RH. The calculated growth factors
244 from a model based on the ZSR relation agree well with the hygroscopic growth factors of initially
245 well-mixed AS/PA particles when accounting for measurement uncertainty. A possible reason for
246 this good agreement is that the measured growth factors referring to the water uptake contribution
247 by PA in the ZSR relation are obtained from the fitted growth curve of pure PA particles (as shown
248 in Fig. 2. Fitted expression, Eq. (1)). Thus, in the case of initially well-mixed AS/PA, relatively good

agreement with the experimental growth factors of mixtures with 25, 50, and 75 wt % PA demonstrates that individual components independently absorb water in proportion to their volume. However, the discrepancy between measured growth factor of initially well-mixed AS/PA particles at 75 % RH and the predicted growth factors by using the ZSR relation may be due to the molecule interaction between organic molecular and completely or partially dissolved AS ions. A similar phenomenon was reported for well-mixed mixtures of AS + levoglucosan in the previous study by Lei et al (2014, 2018). In addition, the use of the AIOMFAC-LLE model to predict LLPS and RH-dependent water content of AS/PA particles containing 46 wt % PA under hydration conditions. As shown in Fig. S3. At low RH, AS forms a crystalline phase prior to its deliquescence. Thus, AS is predominantly partitioned to the solid phase (δ), while PA is found in a separate amorphous/liquid phase that further contains water (in solid−liquid equilibrium) up to the complete AS deliquescence at ∼79 % RH. Two liquid phases, one AS-rich (α) and one PA-rich (β), are predicted to coexist between 79 % < RH < 96 % in the hydration case. At RH above 96 %, a single liquid phase is the stable state. Although, we note that AIOMFAC-LLE may have an uncertainty of several % RH in terms of the RH range in which LLPS is predicted (Song et al., 2012).

3.2 Hygroscopic growth of core-shell-generated structured aerosol particles

Figure 3 shows the measured hygroscopic growth of core-shell-generated structured particles as a function of RH. Here, we investigated the hygroscopic behavior of samples of various AS core particle sizes (AS particle dry diameter of 100, 150, and 200nm) and coating (PA coating of 10, 20, 30, and 50nm), respectively. The core-shell-generated structured particles start to absorb a small amount of water at RH lower than the DRH of AS due to the organic coating. A similar behavior has been observed for core-shell-generated structured particles containing AS and palmitic acid by

Garland et al. (2005), where early water uptake and reduced hygroscopic growth after deliquescence of AS (compared to pure AS aerosols) were reported. A reduction of the hygroscopic growth factors of core-shell-generated particles becomes obvious as the thickness of the PA shell increases after the deliquescence of core-shell-generated particles. For example, the measured growth factor value at 80% RH is 1.45, 1.40, 1.32, and 1.28 for core-shell-generated particles containing 100 nm AS and 10, 20, 30, and 50 nm coating PA shell, respectively. The kinetic limitation on the core-shell-generated particles is expected to increase considerably with increasing the thickness of the coating PA shells, which retards the transport rate of water molecules across core-shell-generated aerosol particles/air interface. In addition, the measured hygroscopic growth factor of core-shell-generated AS/PA mixtures is predicted by the ZSR relation, which is based on the hygroscopic growth factors of AS and PA derived from the E-AIM predictions for AS and the fitted GF curve (Eq. 1). The ZSR-based predictions are lower than that of core-shell-generated aerosol particles at RH in the range of 5 % - 90 %. The underprediction of the ZSR relation was also observed in the literature (Chan et al., 2006; Sjogren et al., 2007). Sjogren et al. (2006) observed an enhanced water uptake of mixtures consisting of AS and adipic acid with different mass ratios (1:2, 1:3, and 1:4) at RH above 80 % compared with ZSR relation in the hydration condition. They assumed that adipic acid is more likely to enclose the water-soluble AS in veins and cavities, which results in easy uptake of water and a negative curvature of the solution meniscus at the opening of the vein compared to a flat or convex particle surface. Therefore, in the case of AS/PA core-shell-generated particles, one potential reason for the underestimation of the measured growth factor by ZSR relation is the morphology effect on the core-shell-generated structured AS/PA particle. To be specific, due to the potential presence of polycrystalline AS, containing pores, cracks, and veins (Zelenyuk et al., 2006; Sjogren et al., 2007),

293 when RH approaches 80 %, these pores or veins may fill with aqueous PA solution. Thus, water
294 molecules may be easier to diffuse to the veins or pores than particle surface. At RH above 80 %,
295 deliquesced AS is more likely to mixed partial aqueous solution PA. The resulting effect of the
296 arrangement and restructuring of core-shell structured particles may change the hygroscopicity,
297 morphology, and mixing state of the core-shell-generated particles (Chan et al., 2006; Sjogren et al.,
298 2007).
299 Figure 4 shows that the experimental water absorption of the varying size of AS core coated with
300 50-nm PA shell in the hydration condition. In the case of 50-nm PA shell coated with a certain size
301 of the AS core (100, 150, and 200 nm) with respect to 68, 55, and 46 wt % PA in the core-shell-
302 generated particles, It exhibits an increase in hygroscopic growth factor of core-shell-generated
303 particles at RH below 80 % as the size of AS core decreases. However, a decrease in hygroscopic
304 growth factor of core-shell-generated mixtures is observed at RH above 80 % with decreasing the
305 size of the AS core. This indicates that the 50-nm PA shell in the core-shell-generated particles have
306 predominantly contributed to the hygroscopic growth of core-shell-generated particles at low RH.
307 At high RH (e.g., after AS deliquescence), however, 50-nm PA coating shows a weak kinetic
308 limitations for water uptake by core-shell-generated particles as the size of AS core increases. For
309 example, the measured growth factor values are 1.28, 1.34, and 1.40 at 80 % RH for 100-200 nm
310 AS core in the mixed particles, respectively. The discrepancy between measured hygroscopic
311 growth factors and predicted hygroscopic growth factors of core-shell-generated particles by ZSR
312 relation, as discussed in Sect. 3.2, is due to the morphology effect. For ZSR prediction, it assumes
313 that volume fraction of AS components is constant according to the ratio of the volume of AS core
314 in the sphere to the volume of a core-shell-generated sphere based on Eq. (3). Without considering

morphology effect, the ZSR prediction results in an underestimation of hygroscopic growth factors of core-shell-generated particles.

3.3 Comparison of core-shell-generated and initially well-mixed AS/PA aerosol particles

Figure 5 shows the hydration curves of different AS cores coated with the different mass fractions of PA loading (shown in the Supporting Information Table S2) in comparison with those of the initially well-mixed with the same PA mass fractions particles, pure AS particles, and pure PA particles in the range of 5 % - 90 % RH. The effect of the coating PA on core-shell-generated particles becomes more pronounced than that of PA in the initially well-mixed particles at RH below 70 % as shown in Fig 5a-b, which leads to higher amounts of water absorption at low RH. However, compared to Fig 5a-b, Fig. 5c shows the hygroscopic growth factors of initially well-mixed AS/PA is slightly higher than that of AS/PA core-shell-generated particles with 46 wt % PA. At 75 % RH, the measured growth factor value of core-shell-generated particles is lower than that of internally well-mixed mixtures in the PA mass fraction range from 68 to 46 wt % due to the mass transfer limitations of water vapor transport to the AS core in the core-shell-generated particles. For the initially well-mixed AS/PA particles, however, partial dissolution of AS into the liquid PA phase may lead to more water uptake by initially well-mixed particles. For example, for the core-shell-generated mixtures with 68 wt % PA loading, the experimental growth factor value is 1.09 at 75 % RH, relative to the growth factor of 1.17 of initially well-mixed mixtures AS/PA. After an abrupt increase in particle diameter of mixed particles, the core-shell-generated AS/PA particles uptake slightly more water than initially well-mixed AS/PA with the same mass fractions of PA as RH increases above 80 %. Accordingly, at high RH, the occurrence of microscopical restructuring of core-shell-generated particles may affect their size. A similar hygroscopic behavior was observed in

337 previous papers (Chan et al., 2006; Sjogren et al., 2007; Maskey et al., 2014). Chan et al. (2006)
338 investigated hygroscopicity of 49 wt % glutaric acid coated on AS core during two continuous
339 hydration cycles: the experimental growth factor of the fresh core-shell of AS and glutaric acid in
340 the first hydration cycle is slightly higher than those in the second hydration cycle with the same
341 mass fractions of glutaric acid. They suggested that the mixing state has changed from core-shell to
342 well-mixed state during the humidification process. Also, a slightly higher growth factor of core-
343 shell particles than that of well-mixed particles was found when comparing the hygroscopic growth
344 factors of 49 wt % glutaric acid coated on AS core with that of well-mixed mixtures of AS with the
345 same mass fractions of glutaric acid from different papers (Choi et al., 2002; Chan et al., 2006).
346 However, a contrasting phenomenon was observed in the previous study (Maskey et al., 2014).
347 Maskey et al. (2014) investigated the hygroscopic behavior of the internal mixtures consisting AS
348 coated with either succinic acid or levoglucosan in the different mixing state with the same volume
349 fractions of organic compounds. The growth factor of core-shell particles consisting of AS and
350 succinic acid is lower than that of the well-mixed particles, while experimental values for core-shell
351 of AS/levoglucosan particles are close to those of the well-mixed mixtures. The possible reasons for
352 the difference between our study and results from Maskey et al. (2014) are physical properties of
353 the organic components, such as hygrosocpicity, viscosity, volatility, and water uptake coefficients.
354 Therefore, different kinds of organic compounds have a different effect in the hygroscopic growth
355 of mixtures, including the core-shell and the well-mixed state. For example, no hygroscopic growth
356 was observed up to 99 % RH for pure succinic acid particles (shown in Fig. S1a). Peng et al. (2001)
357 measured the DRH of succinic acid at 99 % RH using a bulk solution at 24 °C. Also, Henning et al.
358 (2002) observed no hygroscopic growth of soot/succinic acid core-shell particles in the hydration

359 mode using HTDMA. In the case of AS/succinic acid core-shell particles, No water uptake by AS
360 coated succinic acid shell was observed before 80 % RH, while there is a gradual increase in water
361 absorption of core-shell-generated particles prior to the deliquescence of AS with different mass
362 fraction of PA components as shown in Fig 5a-c. This suggested the physical state of shell is solid
363 and liquid for Maskey et al. (2014) and our measurements, respectively. At RH above 80 %, the
364 kinetic limitation on the water vapor uptake through solid shell into the core is more obvious than
365 that through liquid shell into the core (i.e., liquid diffusion coefficient of water vapor is the range of
366 10^{-10} to 10^{-9} m^2 s^{-1}, solid diffusion coefficient of water vapor is the range of 10^{-13}-10^{-14} m^2 s^{-1} at 25°C).
367 This can lead to different hygroscopic behavior of core-shell particles. In the case of
368 AS/levoglucosan measured by Maskey et al. (2014), they found that the slightly higher growth
369 factors for well-mixed particles are than core-shell aerosol particles (88-nm AS core coated by 12-
370 nm levoglucosan). The mass fraction of levoglucosan in the core-shell-generated particles is ~ 29
371 wt %. In our study, AS coated with PA with mass fraction range is between 46 to 68 wt %. Next,
372 using the low mass fraction of PA (e.g., 29 wt %) in core-shell-generated aerosol particles is to be
373 investigated. In addition, for the AS/PA mixture aerosol particles containing 46-68 wt % PA, the
374 measured growth factors of initially well-mixed AS/PA particles are in good agreement with the
375 ZSR relation prediction comparing with that of core-shell-generated AS/PA particles.
376

377 ## 4 Summary and conclusion

378 In this study, we focused on PA to represent common organic compounds produced by various
379 sources, (e.g., vehicles, biomass burning, photo-oxidation). It is found that PA aerosol particles
380 uptake water continuously as RH increases. We further investigated the effect of PA coating on the

hygroscopicity of core-shell-generated aerosol particles. As PA coating thickness increases, the hygroscopic growth factor of AS/PA core-shell-generated particles increases prior to the deliquescence of AS, but the water uptake decreases at RH above 80 %. Furthermore, we compared the hygroscopic behavior of AS/PA core-shell-generated particles with that of AS/PA initially well-mixed particles. Due to mixing state effects, higher hygroscopic growth factors of AS/PA core-shell-generated particles, compared to that of initially well-mixed particles, were observed in this study at RH above 80 %. In addition, the ZSR relation prediction is in good agreement with measured results of AS/PA initially well-mixed particles, but leads to the underestimation of the hygroscopic growth factor of AS/PA core-shell-generated particles at RH above 80 %. We attribute these discrepancies to the morphology effect when AS deliquesces in the core-shell-generated particles. There are a vast number of internally mixed organic-inorganic aerosol particles existing in the atmosphere. The hygroscopicity behavior of mixture particles exhibits variability during RH cycles depending on the chemical composition, size, and mixing state. Humidity cycles may lead to liquid-liquid phase separation, e.g., in the form of core-shell aerosol particles, including at higher RH or in the salt-supersaturated concentration range. Also, due to the different physicochemical properties of organic compounds (e.g., viscosity, solubility, physical state, and morphology), the equilibrium time varies for these organic coated with inorganic aerosol particles. Therefore, potential kinetic limitations in the HTDMA-measured hygroscopicity of core-shell aerosol particles is to be investigated in both humidification and dehumidification conditions.

Data availability

Readers who are interested in the data should contact Ting Lei (ting.lei@mpic.de)

Acknowledgement

This project was supported by The National Key Research and Development Program of China (2017YFC0209500), and the National Natural Science Foundation of China (91544227, 41822703).

Author contributions: W.G.W designed and led the study. W.G.W and T.L assembled the coating-HTDMA. T.L performed the experiments and then wrote the manuscript. W.G.W supported the experiments. All co-authors discussed the results and commented on manuscript.

Reference

Abo Riziq, A., A., Trainic, M., Erlick, C., Segre, E., and Rudich, Y.: Extinction efficiencies of coated absorbing aerosols measured by cavity ring down aerosol spectrometry, Atmos. Chem. Phys., 8, 1823-1833, 2008.

Abo Riziq, A., Erlick, C., Dinar, E., and Rudich, Y.: Optical properties of absorbing and non-absorbing aerosols retrieved by cavity ring down (CRD) spectroscopy, Atmos. Chem. Phys., 7, 1523-1536, 2007.

Ansari, A. S. and Pandis, S. N.: Water Absorption by Secondary Organic Aerosol and Its Effect on Inorganic Aerosol Behavior, Environmental Science & Technology, 34, 71-77, 2000.

Bertram, A. K., Martin, S. T., Hanna, S. J., Smith, M. L., Bodsworth, A., Chen, Q., Kuwata, M., Liu, A., You, Y., and Zorn, S. R.: Predicting the relative humidities of liquid-liquid phase separation, efflorescence, and deliquescence of mixed particles of ammonium sulfate, organic material, and water using the organic-to-sulfate mass ratio of the particle and the oxygen-to-carbon elemental ratio of the organic component, Atmos. Chem. Phys., 11, 10995-11006, 2011.

Brooks, S. D., DeMott, P. J., and Kreidenweis, S. M.: Water uptake by particles containing humic

materials and mixtures of humic materials with ammonium sulfate, Atmospheric Environment, 38, 1859-1868, 2004.

Chan, M. N., Lee, A. K. Y., and Chan, C. K.: Responses of ammonium sulfate particles coated with glutaric acid to cyclic changes in relative humidity: Hygroscopicity and Raman characterization, Environmental Science & Technology, 40, 6983-6989, 2006.

Cheng, Y. F., Wiedensohler, A., Eichler, H., Heintzenberg, J., Tesche, M., Ansmann, A., Wendisch, M., Su, H., Althausen, D., Herrmann, H., Gnauk, T., Brüggemann, E., Hu, M., and Zhang, Y. H.: Relative humidity dependence of aerosol optical properties and direct radiative forcing in the surface boundary layer at Xinken in Pearl River Delta of China: An observation based numerical study, Atmospheric Environment, 42, 6373-6397, 2008.

Choi, M. Y. and Chan, C. K.: The Effects of Organic Species on the Hygroscopic Behaviors of Inorganic Aerosols, Environmental Science & Technology, 36, 2422-2428, 2002.

Ciobanu, V. G., Marcolli, C., Krieger, U. K., Weers, U., and Peter, T.: Liquid−Liquid Phase Separation in Mixed Organic/Inorganic Aerosol Particles, The Journal of Physical Chemistry A, 113, 10966-10978, 2009.

Cruz, C. N. and Pandis, S. N.: Deliquescence and Hygroscopic Growth of Mixed Inorganic−Organic Atmospheric Aerosol, Environmental Science & Technology, 34, 4313-4319, 2000.

Eichler, H., Cheng, Y. F., Birmili, W., Nowak, A., Wiedensohler, A., Brüggemann, E., Gnauk, T., Herrmann, H., Althausen, D., Ansmann, A., Engelmann, R., Tesche, M., Wendisch, M., Zhang, Y. H., Hu, M., Liu, S., and Zeng, L. M.: Hygroscopic properties and extinction of aerosol particles at ambient relative humidity in South-Eastern China, Atmospheric Environment, 42, 6321-6334, 2008.

Falkovich, A. H., Schkolnik, G., Ganor, E., and Rudich, Y.: Adsorption of organic compounds

pertinent to urban environments onto mineral dust particles, Journal of Geophysical Research: Atmospheres, 109, n/a-n/a, 2004.

Ganguly, D., Jayaraman, A., Rajesh, T. A., and Gadhavi, H.: Wintertime aerosol properties during foggy and nonfoggy days over urban center Delhi and their implications for shortwave radiative forcing, Journal of Geophysical Research: Atmospheres, 111, 2006.

Garland, R. M., Wise, M. E., Beaver, M. R., DeWitt, H. L., Aiken, A. C., Jimenez, J. L., and Tolbert, M. A.: Impact of palmitic acid coating on the water uptake and loss of ammonium sulfate particles, Atmos. Chem. Phys., 5, 1951-1961, 2005.

Gupta, D., Kim, H., Park, G., Li, X., Eom, H. J., and Ro, C. U.: Hygroscopic properties of NaCl and NaNO₃ mixture particles as reacted inorganic sea-salt aerosol surrogates, Atmos. Chem. Phys., 15, 3379-3393, 2015.

Hämeri, K., Charlson, R., and Hansson, H.-C.: Hygroscopic properties of mixed ammonium sulfate and carboxylic acids particles, AIChE Journal, 48, 1309-1316, 2002.

Heintzenberg, J., Maßling, A., and Birmili, W.: The connection between hygroscopic and optical particle properties in the atmospheric aerosol, Geophysical Research Letters, 28, 3649-3651, 2001.

Hodas, N., Zuend, A., Mui, W., Flagan, R., and Seinfeld, J.: Influence of particle-phase state on the hygroscopic behavior of mixed organic–inorganic aerosols, Atmospheric Chemistry and Physics, 15, 5027-5045, 2015.

Hori, M., Ohta, S., Murao, N., and Yamagata, S.: Activation capability of water soluble organic substances as CCN, Journal of Aerosol Science, 34, 419-448, 2003.

Huff Hartz, K. E., Tischuk, J. E., Chan, M. N., Chan, C. K., Donahue, N. M., and Pandis, S. N.: Cloud condensation nuclei activation of limited solubility organic aerosol, Atmospheric

Environment, 40, 605-617, 2006.

Jing, B., Tong, S., Liu, Q., Li, K., Wang, W., Zhang, Y., and Ge, M.: Hygroscopic behavior of multicomponent organic aerosols and their internal mixtures with ammonium sulfate, Atmospheric Chemistry and Physics, 16, 4101-4118, 2016.

K., C. M. N. a. C. C.: Mass transfer effects in hygroscopic measurements of aerosol particles, Atmospheric Chemistry and Physics, 2005. 2005.

Kawamura, K. and Ikushima, K.: Seasonal changes in the distribution of dicarboxylic acids in the urban atmosphere, Environmental Science & Technology, 27, 2227-2235, 1993.

Kleindienst, T. E., Smith, D. F., Li, W., Edney, E. O., Driscoll, D. J., Speer, R. E., and Weathers, W. S.: Secondary organic aerosol formation from the oxidation of aromatic hydrocarbons in the presence of dry submicron ammonium sulfate aerosol, Atmos Environ, 33, 3669-3681, 1999.

Kreidenweis, S. M., Koehler, K., DeMott, P. J., Prenni, A. J., Carrico, C., and Ervens, B.: Water activity and activation diameters from hygroscopicity data - Part I: Theory and application to inorganic salts, Atmospheric Chemistry and Physics, 5, 1357-1370, 2005.

Lang-Yona, N., Abo-Riziq, A., Erlick, C., Segre, E., Trainic, M., and Rudich, Y.: Interaction of internally mixed aerosols with light, Physical Chemistry Chemical Physics, 12, 21-31, 2010.

Lei, T., Zuend, A., Cheng, Y., Su, H., Wang, W., and Ge, M.: Hygroscopicity of organic surrogate compounds from biomass burning and their effect on the efflorescence of ammonium sulfate in mixed aerosol particles, Atmos. Chem. Phys., 18, 1045-1064, 2018.

Lei, T., Zuend, A., Wang, W. G., Zhang, Y. H., and Ge, M. F.: Hygroscopicity of organic compounds from biomass burning and their influence on the water uptake of mixed organic ammonium sulfate aerosols, Atmospheric Chemistry and Physics, 14, 1-20, 2014.

491 Lesins, G., Chylek, P., and Lohmann, U.: A study of internal and external mixing scenarios and its
492 effect on aerosol optical properties and direct radiative forcing, Journal of Geophysical Research:
493 Atmospheres, 107, AAC 5-1-AAC 5-12, 2002.
494 Liu, Q., Jing, B., Peng, C., Tong, S., Wang, W., and Ge, M.: Hygroscopicity of internally mixed
495 multi-component aerosol particles of atmospheric relevance, Atmospheric Environment, 125, 69-
496 77, 2016.
497 Liu, X., Gu, J., Li, Y., Cheng, Y., Qu, Y., Han, T., Wang, J., Tian, H., Chen, J., and Zhang, Y.: Increase
498 of aerosol scattering by hygroscopic growth: Observation, modeling, and implications on visibility,
499 Atmospheric Research, 132, 91-101, 2013.
500 Liu, X., Zhang, Y., Cheng, Y., Hu, M., and Han, T.: Aerosol hygroscopicity and its impact on
501 atmospheric visibility and radiative forcing in Guangzhou during the 2006 PRIDE-PRD campaign,
502 Atmospheric Environment, 60, 59-67, 2012.
503 Martin, A. C., Cornwell, G. C., Atwood, S. A., Moore, K. A., Rothfuss, N. E., Taylor, H., DeMott,
504 P. J., Kreidenweis, S. M., Petters, M. D., and Prather, K. A.: Transport of pollution to a remote
505 coastal site during gap flow from California's interior: impacts on aerosol composition, clouds, and
506 radiative balance, Atmos. Chem. Phys., 17, 1491-1509, 2017.
507 Maskey, S., Chong, K. Y., Kim, G., Kim, J.-S., Ali, A., and Park, K.: Effect of mixing structure on
508 the hygroscopic behavior of ultrafine ammonium sulfate particles mixed with succinic acid and
509 levoglucosan, Particuology, 13, 27-34, 2014.
510 Miñambres, L., Sánchez, M. N., Castaño, F., and Basterretxea, F. J.: Hygroscopic Properties of
511 Internally Mixed Particles of Ammonium Sulfate and Succinic Acid Studied by Infrared
512 Spectroscopy, The Journal of Physical Chemistry A, 114, 6124-6130, 2010.

513 Pagels, J., Khalizov, A. F., McMurry, P. H., and Zhang, R. Y.: Processing of Soot by Controlled
514 Sulphuric Acid and Water Condensation—Mass and Mobility Relationship, Aerosol Science and
515 Technology, 43, 629-640, 2009.
516 Peng, C., Chan, M. N., and Chan, C. K.: The Hygroscopic Properties of Dicarboxylic and
517 Multifunctional Acids: Measurements and UNIFAC Predictions, Environmental Science &
518 Technology, 35, 4495-4501, 2001.
519 Qiu, C. and Zhang, R.: Multiphase chemistry of atmospheric amines, Physical Chemistry Chemical
520 Physics, 15, 5738-5752, 2013.
521 Rogge, W. F., Mazurek, M. A., Hildemann, L. M., Cass, G. R., and Simoneit, B. R. T.: Quantification
522 of urban organic aerosols at a molecular level: Identification, abundance and seasonal variation,
523 Atmospheric Environment. Part A. General Topics, 27, 1309-1330, 1993.
524 Rose, D., Gunthe, S. S., Su, H., Garland, R. M., Yang, H., Berghof, M., Cheng, Y. F., Wehner, B.,
525 Achtert, P., Nowak, A., Wiedensohler, A., Takegawa, N., Kondo, Y., Hu, M., Zhang, Y., Andreae, M.
526 O., and Poschl, U.: Cloud condensation nuclei in polluted air and biomass burning smoke near the
527 mega-city Guangzhou, China -Part 2: Size-resolved aerosol chemical composition, diurnal cycles,
528 and externally mixed weakly CCN-active soot particles, Atmospheric Chemistry and Physics, 11,
529 2817-2836, 2011.
530 Rudich, Y.: Laboratory Perspectives on the Chemical Transformations of Organic Matter in
531 Atmospheric Particles, Chemical Reviews, 103, 5097-5124, 2003.
532 Saxena, P., Hildemann, L. M., McMurry, P. H., and Seinfeld, J. H.: Organics alter hygroscopic
533 behavior of atmospheric particles, Journal of Geophysical Research: Atmospheres, 100, 18755-
534 18770, 1995.

535 Schauer, J. J. and Cass, G. R.: Source Apportionment of Wintertime Gas-Phase and Particle-Phase
536 Air Pollutants Using Organic Compounds as Tracers, Environmental Science & Technology, 34,
537 1821-1832, 2000.
538 Schauer, J. J., Fraser, M. P., Cass, G. R., and Simoneit, B. R. T.: Source Reconciliation of
539 Atmospheric Gas-Phase and Particle-Phase Pollutants during a Severe Photochemical Smog
540 Episode, Environmental Science & Technology, 36, 3806-3814, 2002.
541 Schauer, J. J., Rogge, W. F., Hildemann, L. M., Mazurek, M. A., Cass, G. R., and Simoneit, B. R.
542 T.: Source apportionment of airborne particulate matter using organic compounds as tracers,
543 Atmospheric Environment, 30, 3837-3855, 1996.
544 Schwarz, J. P., Gao, R. S., Fahey, D. W., Thomson, D. S., Watts, L. A., Wilson, J. C., Reeves, J. M.,
545 Darbeheshti, M., Baumgardner, D. G., Kok, G. L., Chung, S. H., Schulz, M., Hendricks, J., Lauer,
546 A., Kärcher, B., Slowik, J. G., Rosenlof, K. H., Thompson, T. L., Langford, A. O., Loewenstein, M.,
547 and Aikin, K. C.: Single-particle measurements of midlatitude black carbon and light-scattering
548 aerosols from the boundary layer to the lower stratosphere, Journal of Geophysical Research:
549 Atmospheres, 111, n/a-n/a, 2006.
550 Shi, Y. J., Ge, M. F., and Wang, W. G.: Hygroscopicity of internally mixed aerosol particles
551 containing benzoic acid and inorganic salts, Atmospheric Environment, 60, 9-17, 2012.
552 Shiraiwa, M., Zuend, A., Bertram, A. K., and Seinfeld, J. H.: Gas-particle partitioning of
553 atmospheric aerosols: interplay of physical state, non-ideal mixing and morphology, Physical
554 Chemistry Chemical Physics, 15, 11441-11453, 2013.
555 Sjogren, S., Gysel, M., Weingartner, E., Baltensperger, U., Cubison, M. J., Coe, H., Zardini, A. A.,
556 Marcolli, C., Krieger, U. K., and Peter, T.: Hygroscopic growth and water uptake kinetics of two-

557 phase aerosol particles consisting of ammonium sulfate, adipic and humic acid mixtures, Journal of
558 Aerosol Science, 38, 157-171, 2007.
559 Song, M., Ham, S., Andrews, R. J., You, Y., and Bertram, A. K.: Liquid–liquid phase separation in
560 organic particles containing one and two organic species: importance of the average
561 O : C, Atmos. Chem. Phys., 18, 12075-12084, 2018.
562 Song, M., Marcolli, C., Krieger, U. K., Zuend, A., and Peter, T.: Liquid-liquid phase separation and
563 morphology of internally mixed dicarboxylic acids/ammonium sulfate/water particles, Atmospheric
564 Chemistry and Physics, 12, 2691-2712, 2012a.
565 Song, M., Marcolli, C., Krieger, U. K., Zuend, A., and Peter, T.: Liquid-liquid phase separation in
566 aerosol particles: Dependence on O:C, organic functionalities, and compositional complexity,
567 Geophysical Research Letters, 39, 2012b.
568 Spindler, C., Riziq, A. A., and Rudich, Y.: Retrieval of Aerosol Complex Refractive Index by
569 Combining Cavity Ring Down Aerosol Spectrometer Measurements with Full Size Distribution
570 Information, Aerosol Science and Technology, 41, 1011-1017, 2007.
571 Stock, M., Cheng, Y. F., Birmili, W., Massling, A., Wehner, B., Müller, T., Leinert, S., Kalivitis, N.,
572 Mihalopoulos, N., and Wiedensohler, A.: Hygroscopic properties of atmospheric aerosol particles
573 over the Eastern Mediterranean: implications for regional direct radiative forcing under clean and
574 polluted conditions, Atmos. Chem. Phys., 11, 4251-4271, 2011.
575 Su, H., Rose, D., Cheng, Y. F., Gunthe, S. S., Massling, A., Stock, M., Wiedensohler, A., Andreae,
576 M. O., and Pöschl, U.: Hygroscopicity distribution concept for measurement data analysis and
577 modeling of aerosol particle mixing state with regard to hygroscopic growth and CCN activation,
578 Atmos. Chem. Phys., 10, 7489-7503, 2010.

579 Tang, I. N. and Munkelwitz, H. R.: Water activities, densities, and refractive indices of aqueous
580 sulfates and sodium nitrate droplets of atmospheric importance, Journal of Geophysical Research:
581 Atmospheres, 99, 18801-18808, 1994.
582 Tie, X., Huang, R.-J., Cao, J., Zhang, Q., Cheng, Y., Su, H., Chang, D., Pöschl, U., Hoffmann, T.,
583 Dusek, U., Li, G., Worsnop, D. R., and O'Dowd, C. D.: Severe Pollution in China Amplified by
584 Atmospheric Moisture, Scientific Reports, 7, 15760, 2017.
585 Wang, G., Kawamura, K., Xie, M., Hu, S., Li, J., Zhou, B., Cao, J., and An, Z.: Selected water-
586 soluble organic compounds found in size-resolved aerosols collected from urban, mountain and
587 marine atmospheres over East Asia, Tellus B, 63, 371-381, 2011.
588 Wex, H., Hennig, T., Salma, I., Ocskay, R., Kiselev, A., Henning, S., Massling, A., Wiedensohler,
589 A., and Stratmann, F.: Hygroscopic growth and measured and modeled critical super-saturations of
590 an atmospheric HULIS sample, Geophysical Research Letters, 34, n/a-n/a, 2007.
591 Xue, H., Khalizov, A. F., Wang, L., Zheng, J., and Zhang, R.: Effects of dicarboxylic acid coating
592 on the optical properties of soot, Physical Chemistry Chemical Physics, 11, 7869-7875, 2009.
593 You, Y., Smith, M. L., Song, M., Martin, S. T., and Bertram, A. K.: Liquid–liquid phase separation
594 in atmospherically relevant particles consisting of organic species and inorganic salts, International
595 Reviews in Physical Chemistry, 33, 43-77, 2014.
596 Zamora, I. R., Tabazadeh, A., Golden, D. M., and Jacobson, M. Z.: Hygroscopic growth of common
597 organic aerosol solutes, including humic substances, as derived from water activity measurements,
598 Journal of Geophysical Research: Atmospheres, 116, n/a-n/a, 2011.
599 Zawadowicz, M. A., Proud, S. R., Seppalainen, S. S., and Cziczo, D. J.: Hygroscopic and phase
600 separation properties of ammonium sulfate/organics/water ternary solutions, Atmos. Chem. Phys.,

15, 8975-8986, 2015.

Zelenyuk, A., Cai, Y., and Imre, D.: From Agglomerates of Spheres to Irregularly Shaped Particles: Determination of Dynamic Shape Factors from Measurements of Mobility and Vacuum Aerodynamic Diameters, Aerosol Science and Technology, 40, 197-217, 2006.

Zhang, Q., Canagaratna, M. R., Jayne, J. T., Worsnop, D. R., and Jimenez, J.-L.: Time- and size-resolved chemical composition of submicron particles in Pittsburgh: Implications for aerosol sources and processes, Journal of Geophysical Research: Atmospheres, 110, n/a-n/a, 2005.

Zhang, R., Khalizov, A. F., Pagels, J., Zhang, D., Xue, H., and McMurry, P. H.: Variability in morphology, hygroscopicity, and optical properties of soot aerosols during atmospheric processing, Proceedings of the National Academy of Sciences, 105, 10291-10296, 2008.

Zhang, Y.-L., Kawamura, K., Watanabe, T., Hatakeyama, S., Takami, A., and Wang, W.: New directions: Need for better understanding of source and formation process of phthalic acid in aerosols as inferred from aircraft observations over China, Atmospheric Environment, 140, 147-149, 2016.

Zhou, Q., Pang, S.-F., Wang, Y., Ma, J.-B., and Zhang, Y.-H.: Confocal Raman Studies of the Evolution of the Physical State of Mixed Phthalic Acid/Ammonium Sulfate Aerosol Droplets and the Effect of Substrates, The Journal of Physical Chemistry B, 118, 6198-6205, 2014.

Zuend, A., Marcolli, C., Luo, B. P., and Peter, T.: A thermodynamic model of mixed organic-inorganic aerosols to predict activity coefficients, Atmospheric Chemistry and Physics, 8, 4559-4593, 2008.

Zuend, A., Marcolli, C., Peter, T., and Seinfeld, J. H.: Computation of liquid-liquid equilibria and phase stabilities: implications for RH-dependent gas/particle partitioning of organic-inorganic

aerosols, Atmospheric Chemistry and Physics, 10, 7795-7820, 2010.

Zuend, A. and Seinfeld, J. H.: A practical method for the calculation of liquid–liquid equilibria in multicomponent organic–water–electrolyte systems using physicochemical constraints, Fluid Phase Equilibria, 337, 201-213, 2013.

Tables

Table 1. Coefficients of the fitted growth curve parameterization to measured growth factor data using Eq. (1)

Chemical Compound	a	b	c
Phthalic Acid	0.083116	0.291473	-0.353544

Figures

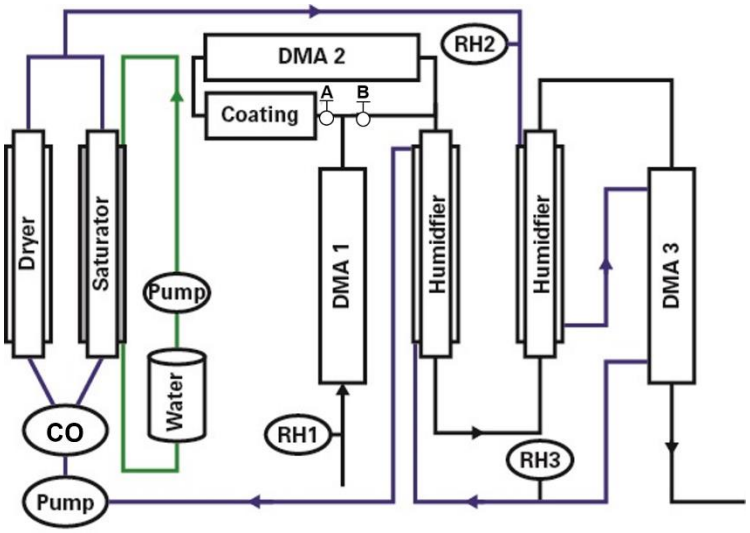

Figure 1. Schematic diagram of the coating-hygroscopicity tandem differential mobility analyzer. Here, CO: critical orifice; DMA: differential mobility analyzer; RH1 and RH2 (measured RH sensor) represent the RH of aerosol and humidified flow in the inlet of DMA1 and humidifier, respectively. RH3 (measured by dew point mirror) represent the RH of excess air. Valve B is open and valve A is closed to the homogeneous internally mixed-mode experiment. Valve A is open and Valve B is closed to the coating-mode experiment. Black line: aerosol line; Blue line: sheath line; Green line: Milli-Q water.

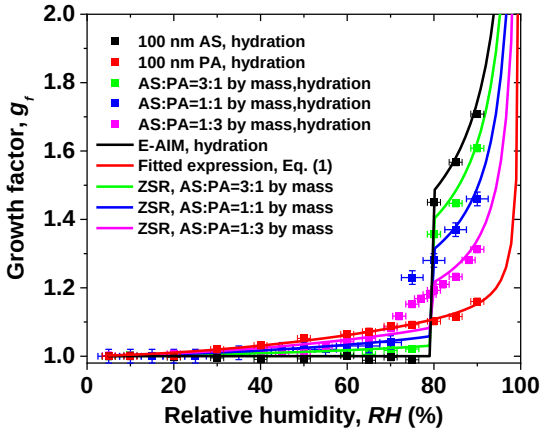

682

683 **Figure 2.** Hygroscopic growth factor for 100 nm (dry diameter, RH < 5 %) aerosol particles containing:

684 ammonium sulfate (AS), phthalic acid (PA), and initially well-mixed mixtures of PA and AS with

685 different mass ratio of AS to PA. In comparison, the E-AIM model, the fitted expression Eq. (1), and the

686 ZSR relation predicted growth factors of AS, PA, and initially well-mixed particles with different mass

687 fractions of PA, respectively.

688

689

690

691

692

693

694

695

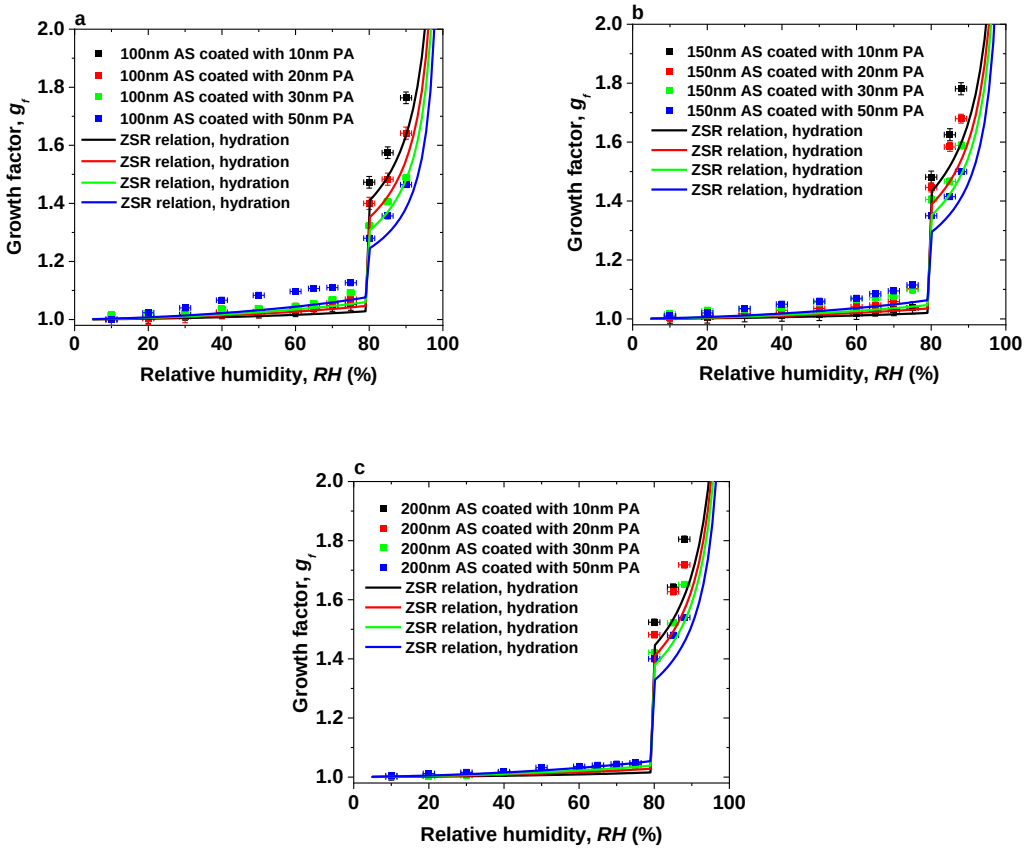

Figure 3. Hygroscopic growth factor for core-shell-generated of ammonium sulfate (AS) and phthalic acid (PA) aerosol particles. In comparison, the ZSR relation predicted growth factor of core-shell-generated aerosol particles (**a**) 100-nm AS core (**b**) 150-nm AS core (**c**) 200-nm AS core.

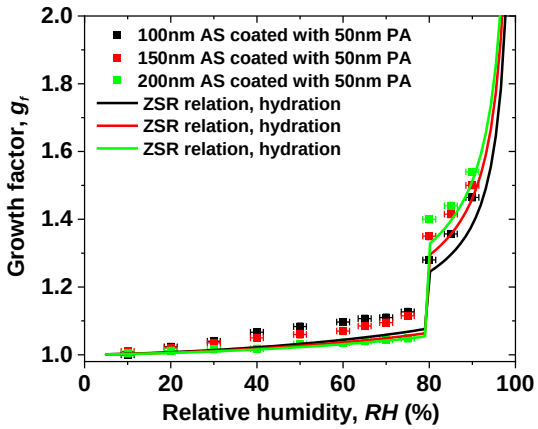

705

706 **Figure 4.** Hygroscopic growth factor for 100-200 nm ammonium sulfate (AS) core with coating 50 nm

707 phthalic acid (PA). In comparison, the ZSR relation predicted growth factor of core-shell-generated

708 aerosol particles with different AS cores.

709

710

711

712

713

714

715

716

717

718

719

720

721

722

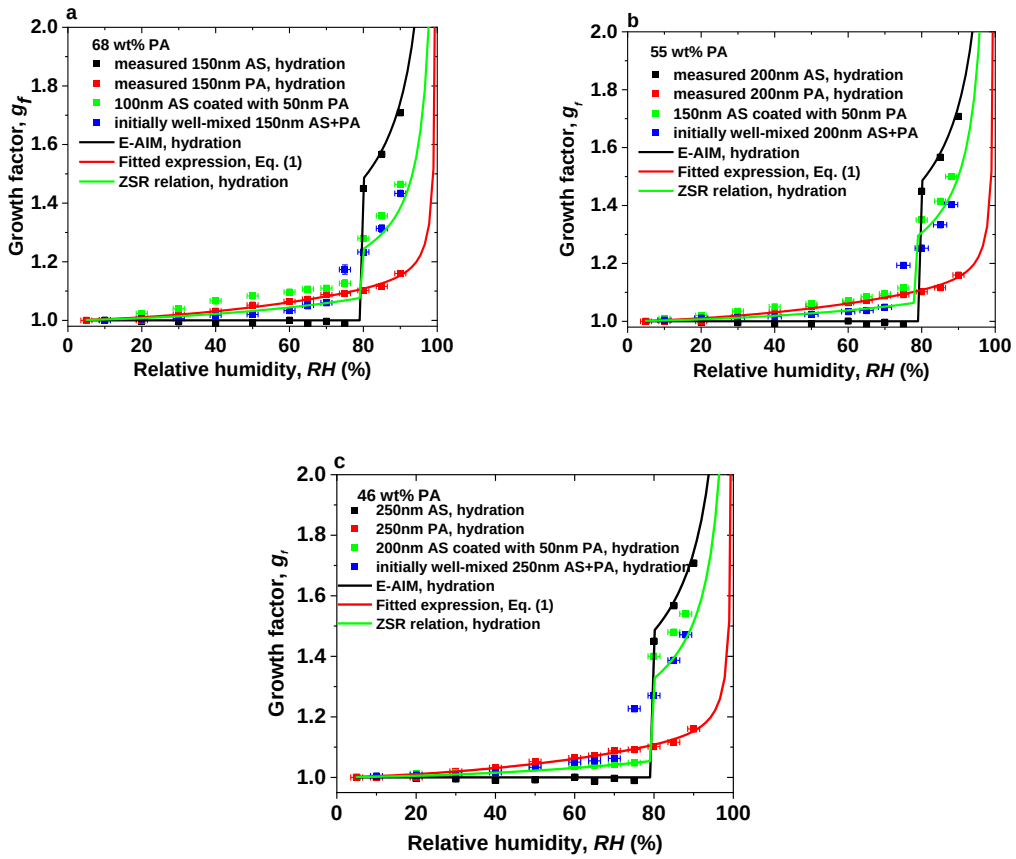

723

724 Figure 5. Hygroscopic growth factor for core-shell-generated and initially well-mixed aerosol particles

725 with the same dry mass fractions of phthalic acid (PA) containing: (a): 68 wt % PA, (b): 55 wt % PA, (c):

726 46 wt % PA. In comparison, the E-AIM model, the fitted expression Eq. (1), and the ZSR relation

727 predicted growth factors of ammonium sulfate (AS), PA, and internally well-mixed particles with

728 different mass fractions of PA, respectively.

729

730